NANO LETTERS

pubs.acs.org/NanoLett

Letter

Quantum Confinement Suppressing Electronic Heat Flow below the Wiedemann–Franz Law

Danial Majidi, Martin Josefsson, Mukesh Kumar, Martin Leijnse, Lars Samuelson, Hervé Courtois, Clemens B. Winkelmann,* and Ville F. Maisi*

Cite This: *Nano Lett.* 2022, 22, 630–635

Read Online

ACCESS | Metrics & More | Article Recommendations | Supporting Information

ABSTRACT: The Wiedemann–Franz law states that the charge conductance and the electronic contribution to the heat conductance are proportional. This sets stringent constraints on efficiency bounds for thermoelectric applications, which seek a large charge conduction in response to a small heat flow. We present experiments based on a quantum dot formed inside a semiconducting InAs nanowire transistor, in which the heat conduction can be tuned significantly below the Wiedemann–Franz prediction. Comparison with scattering theory shows that this is caused by quantum confinement and the resulting energy-selective transport properties of the quantum dot. Our results open up perspectives for tailoring independently the heat and electrical conduction properties in semiconductor nanostructures.

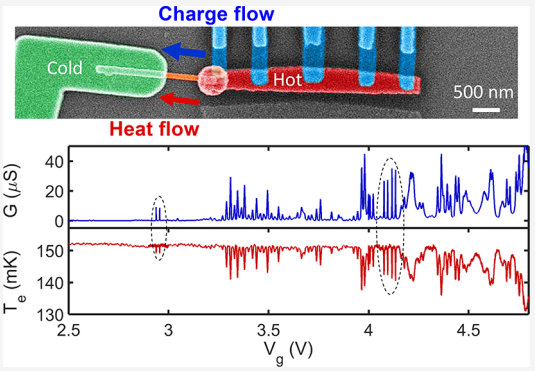

KEYWORDS: *heat transport, quantum dot junction, scattering theory, Wiedemann–Franz law*

In conductors, a higher electrical conductance G is generally associated with a correspondingly higher heat conductance κ. The Wiedemann–Franz (WF) law indeed stipulates that at a given temperature T, the ratio defined as $L = \kappa/GT$ is constant and equal to the Lorenz number $L_0 = (\pi^2/3)(k_B/e)^2$. The connection of the two quantities arises from the fact that the particles responsible for the transport of charge and heat, respectively, and the relevant scattering mechanisms are the same. Experimentally, the WF law has been verified to hold down to the scale of single-atom and molecule contacts.[1,2] When phonon contributions[3] can be neglected, deviations indicate departures from Fermi liquid physics[4] such as found in superconductors,[5] correlated electron systems,[6,7] Majorana modes,[8] or viscous electron flow.[9] In quantum nanodevices, Coulomb interactions and charge quantization were also shown to lead to departures from the WF law.[10−13]

In semiconducting materials, the WF law is usually well obeyed for the electronic contribution to heat conductance, including semiconducting nanostructures displaying transport in the quantum Hall state.[14,15] This property imposes severe limitations for instance in thermoelectrics, for which it is desirable to maximize the charge flow while minimizing that of heat. The most common figure of merit for thermoelectric conversion, $ZT = GS^2T/\kappa$, where S is the Seebeck coefficient, is indeed directly proportional to L^{-1}. Nevertheless, semiconducting nanostructures can display adjustable and strongly energy-selective transport processes, which could also lead to breaking the WF law, even in the absence of interaction effects.[10,16,17] This can be provided for instance by the quantization of the energy levels in a single-quantum-dot junction, allowing for an adjustable narrow transmission window in energy. Although theory has predicted a vanishing L/L_0 for weakly tunnel-coupled quantum dots at low temperature,[18−23] it was experimentally shown that higher-order effects restore a significant electronic heat leakage.[24] The validity of the WF law in a single-quantum-dot device has however not yet been quantitatively investigated because of the difficulty in measuring the extremely small heat currents.

In this work, we investigate heat flow in a quantum dot formed in an InAs nanowire grown by chemical beam epitaxy.[25] Such nanowires have been widely studied for their promising thermoelectric properties.[26−30] It was recognized that the formation of quantum-dot-like states in nanowires can lead to a large enhancement of the thermopower, well beyond expectations from 1D models.[26] Such quantum dots can be produced either by inserting controlled InP tunnel barriers or simply by the inherent electrostatical nonuniformities at a low carrier density. They recently allowed experimentally testing the Curzon–Ahlborn limit of thermoelectric conversion efficiency at maximum power.[31] Although entering directly in

Received: September 6, 2021
Revised: January 12, 2022
Published: January 14, 2022

https://doi.org/10.1021/acs.nanolett.1c03437
Nano Lett. 2022, 22, 630–635

the thermoelectric efficiencies, the electronic heat conductance of such devices is in general not measured independently. Because at temperatures above a few degrees Kelvin, the thermal transport properties of InAs nanowires are known to be strongly dominated by phonons,[32] the *electronic* heat conductance of InAs can only be experimentally probed at milliKelvin temperatures.

The experimental device is an InAs nanowire of 70 nm diameter, back-gated from the degenerately doped silicon substrate at a potential V_g and electrically connected on one side to a large gold contact named *drain* from hereon (Figure 1a). The contact resistance to such nanowires is typically on

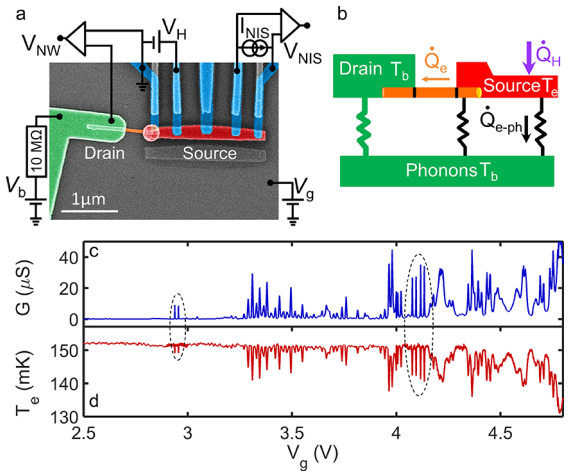

Figure 1. Heat transport experiment through an InAs nanowire device. (a) False-colored scanning electron micrograph of the device. The drain electrode, the source island, and the nanowire are colored in green, red, and orange, respectively. Five superconducting aluminum leads (light blue) are connected to the source island for heating the source side and measuring its electronic temperature. Thermometry is performed by measuring the voltage V_{NIS} at a fixed floating current bias I_{NIS}. (b) Heat balance diagram, which includes the applied power to the source island, $\dot{Q}_H$; the heat escaping due to electron−phonon coupling, $\dot{Q}_{e\text{-}ph}$; and the electronic heat flow along the nanowire, $\dot{Q}_e$. (c) Electrical conductance at thermal equilibrium and (d) temperature response T_e of the source island with the heating power of $\dot{Q}_H$ = 16 fW as a function of the back gate voltage V_g. The dashed ellipses highlight resonances that will be studied in more detail. All measurements are taken at a bath temperature T_b = 100 mK.

the order of a few 100 Ω at most,[33,34] that is, much less than the device resistances that we consider in this work. The nanowire conductance dI/dV_{NW} is measured using a voltage division scheme as pictured in Figure 1a, involving a 10 MΩ bias resistor. The other side (the *source*) consists of a few-micrometer-long normal metallic island, connected by five superconducting aluminum leads. The leftmost of these in Figure 1a is in direct ohmic contact with the source island. This allows measuring directly the nanowire linear charge conductance $G(V_g)$, as shown in Figure 1c. In agreement with previous reports on similar structures,[26] the nanowire conduction is pinched off below $V_g \approx 3$ V. Near the pinch off, the conductance displays sharp resonances, which indicate that the nanowire conduction bottleneck at vanishing charge carrier densities will be provided by a quantum dot forming in the part of the nanowire that is not below the metallic contacts (Figure 1c). Although "unintentional" (in contrast with epitaxially engineered quantum dots[35,36]), these quantum dots display a well-defined level quantization $\delta\varepsilon$, tunnel coupling strengths $\gamma_{s,d}$, and charging energies E_c all three significantly larger than k_BT. Here, k_B is the Boltzmann constant, and T is the experimental working temperature, which is set to T_b = 100 mK at equilibrium. Details of the charge conductance properties, which we extract from full $dI/dV_{NW}(V_{NW}, V_g)$ differential conductance maps, are found in the Supporting Information.

The other four aluminum leads to the source are in contact via tunnel barriers. Such superconductor−insulator−normal metal (NIS) junctions are well-known to provide excellent electron heaters and thermometers in low-temperature experiments.[37] Because at mK temperatures both the electron−phonon coupling in metals and the heat conductance of superconductors are very low, the source island electrons are thermally well insulated, such that the heat flow through the nanowire significantly contributes to the source island's heat balance. This is seen in Figure 1d, in which a constant heating power $\dot{Q}_H$ = 16 fW is provided to the source island via a voltage V_H applied on one tunnel lead. As the gate potential is swept, the variations of the source island electron temperature T_e are strikingly anticorrelated to variations of G. The heat balance of our device is schematized in Figure 1b. Because the source island is overheated with respect to its environment, the gradual opening of electronic conduction channels in the InAs nanowire leads to increased heat flow out of the source island and thus a lowering of T_e.

In the remainder of this work, we investigate quantitatively the nanowire heat conductance properties and compare them to the predictions of both the WF law and the Landauer−Büttiker scattering theory.[38] To this end, it is very insightful to go beyond linear response in $\Delta T = T_e - T_b$, and we thus measure at every gate voltage the full relation $\dot{Q}_H(T_e,V_g)$ between the Joule power $\dot{Q}_H$ applied to the source and its internal equilibrium electronic temperature T_e. Details of the determination of $\dot{Q}_H$ are described in the Supporting Information.

An important issue in the determination of electronic heat flow is the proper identification of the parasitic heat escape via other channels, such as electron−phonon coupling.[37] Unless the latter can be neglected,[14] the comparison to a reference, at which the electronic heat conductance is either assumed to be known,[12] or negligible, is required. We define $\dot{Q}_H(T_e,0)$ measured deep in the insulating regime as an experimental reference which contains all heat escape channels out of the source island other than mediated by the nanowire charge carriers. We stress that this choice does not rely on any thermal model, and we furthermore consider the gate-dependent part of the heat balance, defined as $\dot{Q}(T_e,V_g) = \dot{Q}_H(T_e,V_g) - \dot{Q}_H(T_e,0)$. The magnitude and temperature dependence of $\dot{Q}_H(T_e,0)$ is in good agreement with estimates for the electron−phonon coupling in the metallic parts of the source (see Supporting Information). Surprisingly, we observe that $\dot{Q}(T_e,V_g)$ is slightly gate dependent even before the conducting state sets on. This is readily visible as a slightly negative slope of the $T_e(V_g)$ baseline in Figure 1d. We thus conclude on a minute yet measurable and smoothly gate-dependent contribution to the source electron−phonon coupling from the part of the nanowire below the source, which calls for defining in addition a local reference, as discussed below.

The very first conduction resonance, visible in Figure 1c,d and Figure 2a,b at V_g^0 = 2.938 V, is ideally suited for a *local*

https://doi.org/10.1021/acs.nanolett.1c03437
Nano Lett. 2022, 22, 630−635

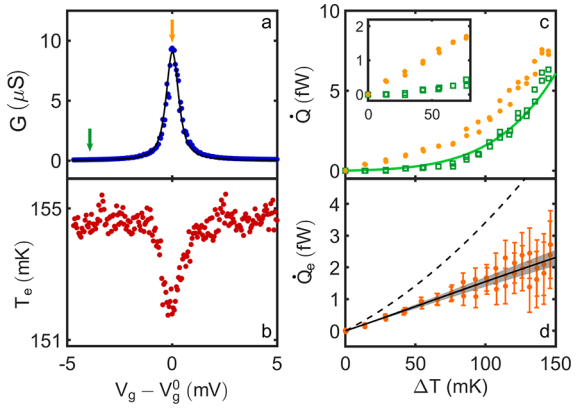

Figure 2. Heat transport near an isolated conductance resonance. (a) Linear charge conductance around V_g^0= 2.938 V at T_b = 100 mK. The black line is a fit using scattering theory. (b) Source temperature T_e as a function of V_g, with a constant applied power $\dot{Q}_H$ = 16 fW, at T_b = 100 mK. (c) Full heat balance curve $\dot{Q}(T_e,V_g)$ on (orange bullets) and off (green squares) the transport resonance, as indicated by the arrows in (a). The green line presents a fit using $\dot{Q} = \beta(T_e^6 - T_b^6)$ with β = 35 ± 5 pW/K^6. The inset highlights the electronic contribution, dominating at the small temperature difference at the resonance. (d) The difference of the two data sets in c, displaying the purely electronic heat transport contribution $\dot{Q}_e$. The dashed and the full lines are the predictions from the WF law and scattering transport theory, respectively. The gray shaded area indicates the uncertainty of the scattering theory calculation, due to the determination of the gate coupling lever arm. The error bars account for the uncertainty in the experimental determination of $\dot{Q}_e$.

background subtraction, revealing the electronic heat conductance $\dot{Q}_e$ through the nanowire on top of the smooth e-ph background contribution $\dot{Q}_{e\text{-}ph}$ of the source side. At gate voltages $|\Delta V_g| \geq 3$ mV away from the conduction resonance at V_g^0, the heat flow $\dot{Q}(T_e,V_g)$ is constant, within noise, although the charge conductance G still varies. After taking the difference of the heat balance on and off resonance (Figure 2c), one is thus left with the quantity of interest, the *electronic* heat flow through the nanowire at resonance, $\dot{Q}_e(T_e,V_g^0) = \dot{Q}(T_e,V_g^0) - \dot{Q}(T_e,V_g^0 + \Delta V_g)$. We stress that this additional background subtraction does not rely on any modeling of the heat balance, such as electron−phonon coupling. As seen in Figure 2d and already visible in the inset of Figure 2c, $\dot{Q}_e$ at V_g^0 displays a strikingly linear dependence on ΔT. We see that the heat conductance $\kappa_e = \partial\dot{Q}_e/\partial T$, that is the initial slope in Figure 2d, differs quantitatively from the WF prediction by a factor $L/L_0 \approx 0.65 \pm 0.1$. Further, beyond linear response, the temperature dependence qualitatively deviates from the parabolic law expected from WF (dashed line).

For a theoretical description beyond the WF law, we use a Landauer−Büttiker noninteracting model, with an energy-dependent transmission $\mathcal{T}(E)$. We write the associated charge and heat currents, respectively as

$$I = \frac{2e}{h}\int_{-\infty}^{\infty} \mathcal{T}(E)\Delta f \, dE \tag{1}$$

and

$$\dot{Q}_e = \frac{2}{h}\int_{-\infty}^{\infty} (E-\mu_s)\mathcal{T}(E)\Delta f \, dE \tag{2}$$

with Δf the difference in the source and drain energy distributions, and μ_s the source island chemical potential.[38,39] The linear charge and heat conductances are then obtained as $G = \partial I/\partial V_{NW}$ and $\kappa_e = \partial\dot{Q}_e/\partial(\Delta T)$, respectively, with $\Delta T = T_e - T_b$. We model each resonance as a discrete energy level coupled to the source and drain reservoirs. We then deduce the transmission function $\mathcal{T}(E)$ by fitting the calculated gate-dependent charge conductance $G(V_g)$ to the data. The accurate determination of $\mathcal{T}(E)$ requires accurately estimating independently the tunnel couplings and the gate lever arm, as both affect similarly the resonance widths. This is described in detail in the Supporting Information. On a technical note, we stress that the above theoretical expression of κ_e assumes open-circuit conditions, that is, no net particle current. For all heat conductance experiments, the nanowire was biased in series with a 10 MΩ resistor at room temperature. Because we only consider data at gate voltages at which G is significantly larger than $(10\ \text{M}\Omega)^{-1} = 0.1\ \mu$S, applying $V_b = 0$ is then equivalent to imposing open circuit conditions.

With the above analysis, the Landauer−Büttiker theoretical $\dot{Q}_e(T_e,V_g)$ follows directly. As seen in Figure 2d (solid black line), the agreement with the experimental data is very good, with no adjustable parameters, reproducing the observed approximately linear dependence on ΔT. The gray shaded region accounts for the uncertainties in the determination of $\mathcal{T}(E)$. The violation of the WF law observed here is therefore accurately described by a noninteracting scattering transport picture.

Intuitively, the deviation from WF at resonance can be understood as stemming from the energy selectivity of the device transmission $\mathcal{T}(E)$, which is a peaked function of width $\gamma = \gamma_s + \gamma_d$, with $\gamma_{s,d}/\hbar$ the tunneling rates between the dot and the source and drain leads, respectively. Only electrons bound at the Fermi level within an energy window of width γ can effectively tunnel, thereby suppressing contributions of the particles from the high-energy tails of the Fermi distribution. Together with a large Seebeck coefficient,[26,27] this relative suppression of heat conductance with respect to the charge conductance makes the quantum dot junction potentially the "best thermoelectric" as theorized by Mahan and Sofo.[40] With increasing tunnel coupling, such that $\gamma > k_BT$, the transmission function $\mathcal{T}(E)$ is broadened, and the energy selectivity is gradually lost, thereby restoring the WF law. A full calculation of L/L_0 versus γ/k_BT is plotted in the Supporting Information, Figure S6.

We exemplify this gradual recovery of the WF law by studying the heat flow close to the conductance resonances observed at a larger gate voltage V_g. While at $V_g \approx 2.9$ V, a ratio $\gamma/k_BT_b \approx 7$ placed the device in the intermediate coupling regime, still displaying sizable energy selectivity (Figure 2), at $V_g \approx 4.1$ V the tunnel couplings are about a factor of 2.5 larger (Figure 3a). We therefore expect a gradual transition to a WF-like heat conductance. This is seen in Figure 3a, where we superimpose the experimentally determined G and κ_e on a vertical scale connecting both quantities via the WF law; that is, $\kappa_e = GT_bL_0$. At the charge degeneracy points (conduction resonances), we observe that the dimensionless reduced heat conductance L/L_0 is now very close to, or barely below, 1. Moving away from the conductance peak, G and κ_e also superimpose nearly exactly, within noise, as also expected from a scattering transport calculation with a now broader $\mathcal{T}(E)$ (line). Observing a sizable deviation from WF requires going beyond linear response (Figure 3b),[41] where the experimental data and the scattering transport calculation remain nevertheless now much closer to the WF law. The main conclusion

https://doi.org/10.1021/acs.nanolett.1c03437
Nano Lett. 2022, 22, 630−635

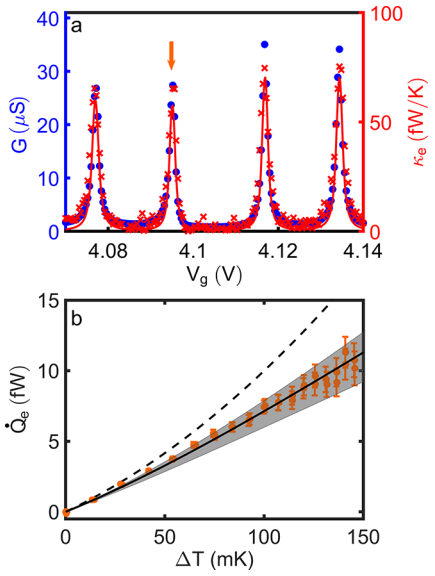

Figure 3. Heat versus charge transport at higher transmissions. (a) Heat (red crosses, right vertical scale) and charge (blue bullets, left vertical scale) conductance resonances at higher transmissions. The ratio of both vertical scales is set to T_bL_0, such that superimposed curves are indicative of the WF law being valid. The red line is the calculated κ_e from scattering transport theory. The L/L_0 for the four peaks are 0.99, 0.97, 0.87, and 0.90 (±0.05) from left to right. (b) $\dot{Q}_e(T_e)$ curve taken at the conduction resonance at V_g = 4.095 V (arrow in (a)). The dashed and the full lines are the predictions from the WF law and scattering transport theory, respectively. The gray shaded area indicates the uncertainty of the scattering theory calculation, due to the determination of the gate coupling lever arm. The error bars account for the uncertainty in the experimental determination of $\dot{Q}_e$.

we draw here is that for increasing tunnel couplings, the scattering theory still describes the experimental data very accurately and over a large temperature difference range. In the linear response regime (small ΔT), the WF law and scattering theory yield convergent predictions.

Moving to yet larger gate voltages (V_g > 4.5 V) and thus electronic transmissions, the charge conductance no longer vanishes in between conduction resonances, impeding the identification of a clear-cut local reference $\dot{Q}_{e\text{-}ph}(T_e)$. This prevents a quantitative separation of the electronic heat flow through the nanowire from the e-ph contribution.

At the lower gate voltages, we however can estimate the e-ph coupling induced by adding carriers to the nanowire segment below the source. This is precisely captured by the off-resonance $\dot{Q}(T_e)$ shown by the green line in Figure 2c, which follows a power law $\propto (T_e^6 - T_b^6)$. Interestingly, this leads to an e-ph coupling constant comparable to that of a metal, in spite of the electron density being several orders of magnitude smaller. This finding is consistent with the strong e-ph coupling found in InAs above 1 K[32] possibly due to piezoelectricity[42] and/or a lateral-confinement-enhanced peaked density of states.[43] We observe the e-ph contribution to change linearly with V_g (see associated plot and analysis in the Supporting Information) implying that the e-ph coupling constant is proportional to the charge carrier density.

In summary, our study reveals a large conjunct evolution in the thermal and charge conductances of an InAs nanowire near pinch off. Around conductance resonances in the quantum dot regime of the nanowire, the heat conductance is significantly lower than expected from the WF law, with $\kappa_e/(GTL_0)$ reaching 0.65 in the intermediate coupling regime, in good agreement with a scattering transport calculation. As anticipated by theory,[40] this establishes experimentally the huge potential of semiconductor nanowires and more generally quantum dot transistors, as promising high-figure-of-merit thermoelectrics. It is interesting to note that while the single-electron transistor (SET) and the quantum-dot junction share extremely similar charge conductance properties in the linear regime, their thermal transport properties show striking differences. At resonance (charge degeneracy), interaction effects are canceled in both types of devices, and the SET thus behaves as a simple metallic heat conductor, whereas the quantum dot junction displays a heat conductance suppression below the WF law. Off resonance, however, Coulomb blockade leads the SET to behave like a high-pass filter in energy (as opposed to the single quantum level, which can be viewed as a band-pass filter), which leads to a heat conductance exceeding the WF law.[11,12] A fascinating open question resides in the role played by electron interactions and correlations in quantum dots,[7,19] which are also expected to lead to marked deviations from the here-employed scattering transport picture, away from the conduction resonances.

■ ASSOCIATED CONTENT

Supporting Information

The Supporting Information is available free of charge at https://pubs.acs.org/doi/10.1021/acs.nanolett.1c03437.

Additional information about the sample fabrication, the electron thermometry, the scattering transport calculations, the determination of the quantum dot parameters, and the analysis of the heat balance (PDF)

■ AUTHOR INFORMATION

Corresponding Authors

Clemens B. Winkelmann − *Université Grenoble Alpes, CNRS, Grenoble INP, Institut Néel, 38042 Grenoble, France;* orcid.org/0000-0003-4320-994X; Email: clemens.winkelmann@neel.cnrs.fr

Ville F. Maisi − *NanoLund and Solid State Physics, Lund University, 22100 Lund, Sweden;* orcid.org/0000-0003-4723-7091; Email: ville.maisi@ftf.lth.se

Authors

Danial Majidi − *Université Grenoble Alpes, CNRS, Grenoble INP, Institut Néel, 38042 Grenoble, France;* orcid.org/0000-0003-4002-8414

Martin Josefsson − *NanoLund and Solid State Physics, Lund University, 22100 Lund, Sweden*

Mukesh Kumar − *NanoLund and Solid State Physics, Lund University, 22100 Lund, Sweden*

Martin Leijnse − *NanoLund and Solid State Physics, Lund University, 22100 Lund, Sweden*

Lars Samuelson − *NanoLund and Solid State Physics, Lund University, 22100 Lund, Sweden;* orcid.org/0000-0003-1971-9894

Hervé Courtois − *Université Grenoble Alpes, CNRS, Grenoble INP, Institut Néel, 38042 Grenoble, France;* orcid.org/0000-0002-3201-9510

Complete contact information is available at: https://pubs.acs.org/10.1021/acs.nanolett.1c03437

https://doi.org/10.1021/acs.nanolett.1c03437
Nano Lett. 2022, 22, 630−635

Author Contributions

V.M. made the devices and performed the experiments. D.M. analyzed the data, with help from all authors. M.K. and L.S. grew the nanowires. M.J. and M.L. performed the theoretical calculations. All authors contributed to the interpretation of the data and writing the manuscript.

Funding

This work received support from the European Union under the Marie Sklodowska-Curie Grant Agreement No. 766 025, the Swedish Research Council, and NanoLund.

Notes

The authors declare no competing financial interest.

All data described here will be made publicly available on Zenodo.

■ ACKNOWLEDGMENTS

We acknowledge insightful discussions with Heiner Linke, Nicola Lo Gullo, Jukka Pekola, and Peter Samuelsson.

■ REFERENCES

(1) Cui, L.; Jeong, W.; Hur, S.; Matt, M.; Klöckner, J. C.; Pauly, F.; Nielaba, P.; Cuevas, J. C.; Meyhofer, E.; Reddy, P. Quantized thermal transport in single-atom junctions. *Science* **2017**, *355*, 1192−1195.

(2) Mosso, N.; Drechsler, U.; Menges, F.; Nirmalraj, P.; Karg, S.; Riel, H.; Gotsmann, B. Heat transport through atomic contacts. *Nat. Nanotechnol.* **2017**, *12*, 430−433.

(3) Lavasani, A.; Bulmash, D.; Das Sarma, S. Wiedemann-Franz law and Fermi liquids. *Phys. Rev. B* **2019**, *99*, 085104.

(4) Benenti, G.; Casati, G.; Saito, K.; Whitney, R. S. Fundamental aspects of steady-state conversion of heat to work at the nanoscale. *Phys. Rep.* **2017**, *694*, 1−124.

(5) Ambegaokar, V.; Tewordt, L. Theory of the electronic thermal conductivity of superconductors with strong electron-phonon coupling. *Phys. Rev.* **1964**, *134*, A805.

(6) Lee, S.; Hippalgaonkar, K.; Yang, F.; Hong, J.; Ko, C.; Suh, J.; Liu, K.; Wang, K.; Urban, J. J.; Zhang, X.; Dames, C.; Hartnoll, S. A.; Delaire, O.; Wu, J. Anomalously low electronic thermal conductivity in metallic vanadium dioxide. *Science* **2017**, *355*, 371−374.

(7) Eckern, U.; Wysokiński, K. I. Charge and heat transport through quantum dots with local and correlated-hopping interactions. *Phys. Rev. Research* **2021**, *3*, 043003.

(8) Pan, H.; Sau, J. D.; Das Sarma, S. Three-terminal nonlocal conductance in Majorana nanowires: Distinguishing topological and trivial in realistic systems with disorder and inhomogeneous potential. *Phys. Rev. B* **2021**, *103*, 014513.

(9) Crossno, J.; Shi, J. K.; Wang, K.; Liu, X.; Harzheim, A.; Lucas, A.; Sachdev, S.; Kim, P.; Taniguchi, T.; Watanabe, K.; Ohki, T. A.; Fong, K. C. Observation of the Dirac fluid and the breakdown of the Wiedemann-Franz law in graphene. *Science* **2016**, *351*, 1058−1061.

(10) Chiatti, O.; Nicholls, J.; Proskuryakov, Y.; Lumpkin, N.; Farrer, I.; Ritchie, D. Quantum thermal conductance of electrons in a one-dimensional wire. *Phys. Rev. Lett.* **2006**, *97*, 056601.

(11) Kubala, B.; König, J.; Pekola, J. P. Violation of the Wiedemann-Franz law in a single-electron transistor. *Phys. Rev. Lett.* **2008**, *100*, 066801.

(12) Dutta, B.; Peltonen, J. T.; Antonenko, D. S.; Meschke, M.; Skvortsov, M. A.; Kubala, B.; König, J.; Winkelmann, C. B.; Courtois, H.; Pekola, J. P. Thermal conductance of a single-electron transistor. *Phys. Rev. Lett.* **2017**, *119*, 077701.

(13) Sivre, E.; Anthore, A.; Parmentier, F. D.; Cavanna, A.; Gennser, U.; Ouerghi, A.; Jin, Y.; Pierre, F. Heat Coulomb blockade of one ballistic channel. *Nat. Phys.* **2018**, *14*, 145−148.

(14) Jézouin, S.; Parmentier, F. D.; Anthore, A.; Gennser, U.; Cavanna, A.; Jin, Y.; Pierre, F. Quantum limit of heat flow across a single electronic channel. *Science* **2013**, *342*, 601−604.

(15) Banerjee, M.; Heiblum, M.; Umansky, V.; Feldman, D. E.; Oreg, Y.; Stern, A. Observation of half-integer thermal Hall conductance. *Nature* **2018**, *559*, 205−210.

(16) Proetto, C. R. Heat conduction through ballistic quantum-point contacts: Quantized steps in the thermal conductance. *Solid State Commun.* **1991**, *80*, 909−912.

(17) Molenkamp, L.; Gravier, T.; Van Houten, H.; Buijk, O.; Mabesoone, M.; Foxon, C. Peltier coefficient and thermal conductance of a quantum point contact. *Phys. Rev. Lett.* **1992**, *68*, 3765.

(18) Zianni, X. Coulomb oscillations in the electron thermal conductance of a dot in the linear regime. *Phys. Rev. B* **2007**, *75*, 045344.

(19) Krawiec, M.; Wysokiński, K. I. Thermoelectric effects in strongly interacting quantum dot coupled to ferromagnetic leads. *Phys. Rev. B* **2006**, *73*, 075307.

(20) Krawiec, M.; Wysokiński, K. I. Thermoelectric phenomena in a quantum dot asymmetrically coupled to external leads. *Phys. Rev. B* **2007**, *75*, 155330.

(21) Murphy, P.; Mukerjee, S.; Moore, J. Optimal thermoelectric figure of merit of a molecular junction. *Phys. Rev. B* **2008**, *78*, 161406.

(22) Tsaousidou, M.; Triberis, G. P. Thermoelectric properties of a weakly coupled quantum dot: enhanced thermoelectric efficiency. *J. Phys.: Cond. Matt.* **2010**, *22*, 355304.

(23) Erdman, P. A.; Mazza, F.; Bosisio, R.; Benenti, G.; Fazio, R.; Taddei, F. Thermoelectric properties of an interacting quantum dot based heat engine. *Phys. Rev. B* **2017**, *95*, 245432.

(24) Dutta, B.; Majidi, D.; Talarico, N. W.; Lo Gullo, N.; Courtois, H.; Winkelmann, C. B. Single-Quantum-Dot Heat Valve. *Phys. Rev. Lett.* **2020**, *125*, 237701.

(25) Fasth, C.; Fuhrer, A.; Samuelson, L.; Golovach, V. N.; Loss, D. Direct measurement of the spin-orbit interaction in a two-electron InAs nanowire quantum dot. *Phys. Rev. Lett.* **2007**, *98*, 266801.

(26) Wu, P. M.; Gooth, J.; Zianni, X.; Svensson, S. F.; Gluschke, J. G.; Dick, K. A.; Thelander, C.; Nielsch, K.; Linke, H. Large thermoelectric power factor enhancement observed in InAs nanowires. *Nano Lett.* **2013**, *13*, 4080−4086.

(27) Roddaro, S.; Ercolani, D.; Safeen, M. A.; Suomalainen, S.; Rossella, F.; Giazotto, F.; Sorba, L.; Beltram, F. Giant thermovoltage in single InAs nanowire field-effect transistors. *Nano Lett.* **2013**, *13*, 3638−3642.

(28) Chen, I.-J.; Burke, A.; Svilans, A.; Linke, H.; Thelander, C. Thermoelectric power factor limit of a 1D nanowire. *Phys. Rev. Lett.* **2018**, *120*, 177703.

(29) Svilans, A.; Josefsson, M.; Burke, A. M.; Fahlvik, S.; Thelander, C.; Linke, H.; Leijnse, M. Thermoelectric characterization of the Kondo resonance in nanowire quantum dots. *Phys. Rev. Lett.* **2018**, *121*, 206801.

(30) Prete, D.; Erdman, P. A.; Demontis, V.; Zannier, V.; Ercolani, D.; Sorba, L.; Beltram, F.; Rossella, F.; Taddei, F.; Roddaro, S. Thermoelectric conversion at 30 K in InAs/InP nanowire quantum dots. *Nano Lett.* **2019**, *19*, 3033−3039.

(31) Josefsson, M.; Svilans, A.; Burke, A. M.; Hoffmann, E. A.; Fahlvik, S.; Thelander, C.; Leijnse, M.; Linke, H. A quantum-dot heat engine operating close to the thermodynamic efficiency limits. *Nat. Nanotechnol.* **2018**, *13*, 920−924.

(32) Matthews, J.; Hoffmann, E. A.; Weber, C.; Wacker, A.; Linke, H. Heat flow in InAs/InP heterostructure nanowires. *Phys. Rev. B* **2012**, *86*, 174302.

(33) Thelander, C.; Björk, M.; Larsson, M.; Hansen, A.; Wallenberg, L.; Samuelson, L. Electron transport in InAs nanowires and heterostructure nanowire devices. *Solid State Commun.* **2004**, *131*, 573−579.

(34) Hansen, A. E.; Björk, M. T.; Fasth, C.; Thelander, C.; Samuelson, L. Spin relaxation in InAs nanowires studied by tunable weak antilocalization. *Phys. Rev. B* **2005**, *71*, 205328.

(35) Björk, M. T.; Thelander, C.; Hansen, A. E.; Jensen, L. E.; Larsson, M. W.; Wallenberg, L. R.; Samuelson, L. Few-electron quantum dots in nanowires. *Nano Lett.* **2004**, *4*, 1621−1625.

https://doi.org/10.1021/acs.nanolett.1c03437
Nano Lett. 2022, 22, 630−635

(36) Dick, K. A.; Thelander, C.; Samuelson, L.; Caroff, P. Crystal phase engineering in single InAs nanowires. *Nano Lett.* **2010**, *10*, 3494−3499.
(37) Giazotto, F.; Heikkilä, T. T.; Luukanen, A.; Savin, A. M.; Pekola, J. P. Opportunities for mesoscopics in thermometry and refrigeration: Physics and applications. *Rev. Mod. Phys.* **2006**, *78*, 217.
(38) Sivan, U.; Imry, Y. Multichannel Landauer formula for thermoelectric transport with application to thermopower near the mobility edge. *Phys. Rev. B* **1986**, *33*, 551.
(39) Davies, J. H. *The Physics of Low-Dimensional Semiconductors: An Introduction*; Cambridge University Press: Cambridge, 1998.
(40) Mahan, G. D.; Sofo, J. O. The best thermoelectric. *Proc. Nat. Acad. Sci.* **1996**, *93*, 7436−7439.
(41) López, R.; Sánchez, D. Nonlinear heat transport in mesoscopic conductors: Rectification, Peltier effect, and Wiedemann-Franz law. *Phys. Rev. B* **2013**, *88*, 045129.
(42) Prasad, C.; Ferry, D. K.; Wieder, H. H. Energy relaxation studies in $In_{0.52}Al_{0.48}As$/ $In_{0.53}Ga_{0.47}As/In_{0.52}Al_{0.48}As$ two-dimensional electron gases and quantum wires. *Semicond. Sci. Technol.* **2004**, *19*, S60.
(43) Sugaya, T.; Bird, J. P.; Ferry, D. K.; Sergeev, A.; Mitin, V.; Jang, K.-Y.; Ogura, M.; Sugiyama, Y. Experimental studies of the electron−phonon interaction in InGaAs quantum wires. *Appl. Phys. Lett.* **2002**, *81*, 727−729.

https://doi.org/10.1021/acs.nanolett.1c03437
Nano Lett. 2022, 22, 630−635